PHYSICAL REVIEW C VOLUME 14, NUMBER 3 SEPTEMBER 1976

# Levels of $^{129}$I populated in the decay of $^{129}$Te$^m$ and $^{129}$Te$^g$

L. G. Mann, W. B. Walters,* and R. A. Meyer
*Lawrence Livermore Laboratory, University of California, Livermore, California 94550*

(Received 17 May 1976)

We have studied the decay of 33-day $^{129}$Te$^m$ and 70-min $^{129}$Te$^g$ with high resolution Ge(Li) detectors used both singly and in coincidence. Sources of $^{129}$Te$^m$ and $^{129}$Te$^g$ in equilibrium were used as well as sources of $^{129}$Te$^g$ containing less than 0.0003 parts $^{129}$Te$^m$ activity. Fifty $\gamma$ rays resulting from $^{129}$Te$^g$ decay and 39 $\gamma$ rays from $^{129}$Te$^m$ decay have been assigned to levels in $^{129}$I. This work establishes new levels in $^{129}$I at 1047.44 ($3/2^+$), 1203.7 ($7/2^+$), 1209.9 ($1/2^+$), and 1282.00 ($7/2^+$) keV ($J^\pi$ in parentheses). In conjunction with recent ($^3$He, $d$) and angular distribution work several other new or more reliable spin-parity assignments can be made as follows: 845 ($9/2^+$), 1112 ($5/2^+$), 1261 ($5/2^+$), 1292 ($3/2^+$), and 1401 ($11/2^-$). The data are discussed in terms of the particle or quasiparticle phonon model and the three-particle cluster model.

RADIOACTIVITY $^{129}$Te [from $^{128}$Te$(n,\gamma)$]; measured $E_\gamma$, $I_\gamma$, $\gamma\gamma$ coin; deduced log*ft*. $^{129}$I deduced levels $E$, $J$, $\Pi$; $B(E2)$. Ge(Li) detectors, enriched $^{128}$Te targets.

## I. INTRODUCTION

The study of the level structure of the odd-mass Sb, I, and Cs nuclides has provided important data in the general understanding of nondeformed nuclei. The levels of the Sb nuclides ($Z=51$) have yielded information that has always been interpreted in the context of a single particle interacting with the closed shell core at $Z=50$. On the other hand, it has been possible to view the I nuclides as a single particle interacting with the $Z=52$ Te core or as a three-particle cluster interacting with the $Z=50$ Sn closed shell. For the Cs nuclides, the distance from the $Z=50$ closed shell has left only a highly collective approach possible.

Among the I nuclides, $^{129}$I has proved to be one of the more attractive for detailed and varied study. Radioactive decay studies have been reported by Bemis and Fransson,[1] Berzins, *et al.*,[2] Dickinson, Bloom, and Mann,[3] Walters and Meyer,[4] Mann, Walters, and Meyer,[5] and DeRaedt, Rots, and Van de Voorde,[6] the latter including angular correlations. Anisotropies in the $\gamma$ decay of oriented nuclei have been reported by Silverans, Schoeters, and Vanneste.[7] Coulomb excitation has been studied by Renwick *et al.*,[8] and the $^{128}$Te($^3$He, $d$)$^{129}$I reaction has been studied by Auble, Ball, and Fulmer.[9] The data up to 1972 have been reviewed by Horen.[10]

Theoretical work on iodine levels in general and for $^{129}$I specifically has been reported by Kisslinger and Sorensen,[11] Heyde and Brussaard,[12] Rustigi, Lucas, and Mukherjee,[13] Almar, Civitarese, and Krmpotic,[14] Vanden Berghe,[15] and A. Kuriyama *et al.*[16]

In this paper we report the results of detailed studies of the $\gamma$-ray spectrum of 33-day $^{129}$Te$^m$-$^{129}$Te$^g$ equilibrium sources as well as studies of 70-min $^{129}$Te$^g$ sources with very little $^{129}$Te$^m$ present. These investigations were stimulated by discrepancies in the spins, parities, and decay character of levels near 560, 1050, and 1400 keV that existed in the earlier works. They are part of a program of systematic studies of odd-proton nuclei.[17]

## II. EXPERIMENTAL PROCEDURES AND RESULTS

### A. Coincidence system

$\gamma$-ray coincidences were studied using two coaxial open-ended Ge(Li) detectors of approximately 40 cm$^3$ each. Two-parameter data were sorted and stored on-line using a PDP-9 computer with 8192 words of core memory and a $2^{20}$-word disk. The conceptual design of this data system has been reported previously.[18] Its utility in this and several other studies warrants a brief description here.

In utilizing a disk as the memory for a conventional multichannel analyzer, the slow access time presents a problem. One can circumvent this problem by using a head-per-track disk and by organizing and temporarily storing in core the incoming data according to their sector address on the disk. This approach successfully handles data rates of several hundred per second while avoiding the need for large amounts of core memory buffering.[19] The accumulated data are available at all times within a matter of a few seconds for CRT display or other forms of readout, such as teletype or magnetic tape. All the problems and delays associated with off-line computer sorting of data stored event by event on magnetic tape are eliminated.

With a $2^{20}$-word memory, two-parameter data can be analyzed with 1024 channels on each parameter and stored completely in a 1024 by 1024 memory array. However, the two pulse heights $x$ and $y$ obtained in our $\gamma$-$\gamma$ coincidence experiments will always have $x+y \leq Q_\beta$. Hence we can digitize one detector output into 1024 channels and the other into 2048 channels and still store all coincidence events in a $2^{20}$-word memory, for the case where each detector is calibrated to accept the full decay energy $Q_\beta$. This was chosen as our standard mode of operation. Figure 1 illustrates how our $2^{20}$-channel stored data field is related to the full data field in general. If $Q_\beta = 2048$ channels in the $Y$ detector and 1024 channels in the $X$ detector, then all possible coincident events will be stored. Otherwise, only the data below the dashed line are stored.

The spectrum in either detector in coincidence with any specified energy window on the other detector can be assembled in core within a few seconds. Up to four such windows may be specified at one time and their resultant coincidence spectra added or subtracted so that the effect of Compton continuum in the energy windows can be eliminated from the final assembled spectrum. These spectra are normally transferred to magnetic tape for analysis and plotting at the computer center, using our standard methods.[20] Magnetic tape is also used for permanent storage of the entire disk records.

Our coincidence system electronics logic is standard. A time-to-amplitude converter (TAC) is used in conjunction with two single-channel (SCA) windows for coincidence selection to permit subtraction of accidental coincidence events during data accumulation. The SCA windows were set at approximately the full width at 0.1 maximum (~100 ns) of the TAC prompt timing output with the $^{129}$Te sources.

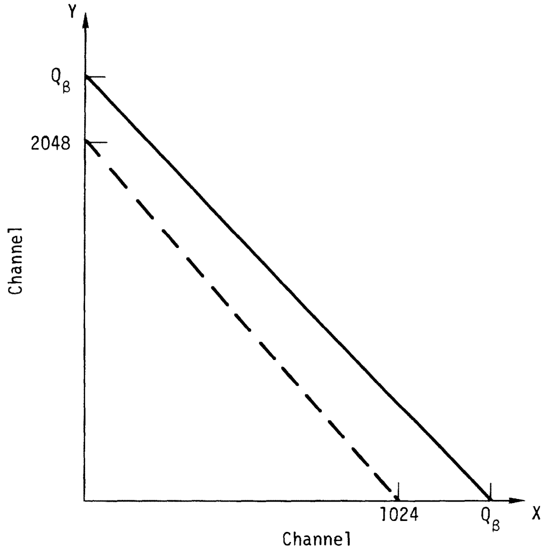

FIG. 1. The data field (below the solid line) of $\gamma$-$\gamma$ coincidences for a maximum decay energy of $Q_\beta$ and the field (below the dashed line) stored in our $2^{20}$-channel data system.

### B. Studies of 70-min $^{129}$Te$^g$

Sources were prepared by irradiating 105 mg of Te metal enriched to 99.5% $^{128}$Te for 60 min in the Livermore Pool Type Reactor (LPTR) at a flux of $1.5\times10^{13}$ $n\,\text{cm}^{-2}\text{s}^{-1}$. This produced sources in which the initial ratio of 70-min to 33-day activities was $\gtrsim$4000. A series of nine samples was studied using Ge(Li) spectroscopy. The first spectrum on each sample was obtained with the Compton suppression system (CSS) described elsewhere.[21] At 1-h intervals a fresh sample was ready for the CSS, and the older sample was transferred to a second detector where it was counted with a number of sources whose $\gamma$-ray energies are well known. This yielded a precise determination of the 560-keV $\gamma$-ray energy, unimpeded by the tail of the much more intense 556-keV $\gamma$ ray normally present in the equilibrium sources previously used (Fig. 2). At later times the sources were again examined with Ge(Li) spectroscopy to check for proper decay half-lives. We list in Table I the energies and intensities of the $\gamma$ rays observed in 70-min $^{129}$Te$^g$ decay.

### C. Studies of equilibrium $^{129}$Te$^{m-g}$

Sources of 33-day $^{129}$Te$^m$ were prepared by a 13-h irradiation in the core of the LPTR at a flux of $7\times10^{13}$ $n\,\text{cm}^{-2}\text{s}^{-1}$. After the decay of 30-h $^{131}$Te$^m$, part of the source was purified chemically and used for both $\gamma$-ray singles and coincidence

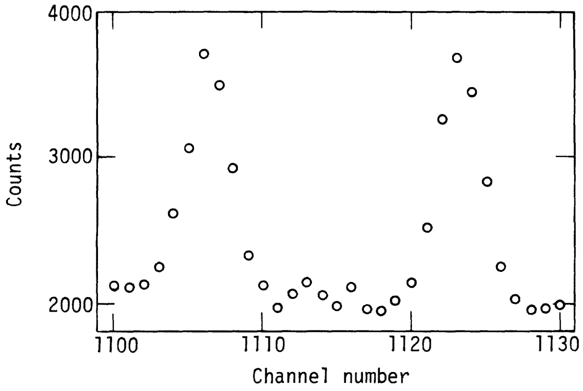

FIG. 2. The 560.05-keV and the unresolved 552.0- and 551.5-keV $\gamma$-ray peaks observed with a Ge(Li) Compton suppression spectrometer and a $^{129}$Te$^g$ source.

TABLE I. $\gamma$-ray energies and intensities following decay of $^{129}$Te$^{g}$.

| $E_\gamma(\Delta E_\gamma)$ (keV) | $I_\gamma(\Delta I_\gamma)$ Singles [b] | | Coinc. gate (keV) | Assignment | |
|---|---|---|---|---|---|
| | | Coincidence | | | |
| 27.814 | ··· | ··· | ··· | 28 | g.s. |
| 208.960(15) | 2.34(1) | 2.34 [c] | 251 | 487 | 278 |
| 210.66(18) | 0.017(9) | 0.019(2) | 1022<br>+<br>1050 | 1261 | 1050 |
| 242.2(–) | 0.0002 [d] | ··· | | 730 | 487 |
| 250.615(15) | 4.97(2) | ··· | ··· | 278 | 28 |
| 270.37(4) | 0.060(4) | 0.068(5) | 532 | 830 | 560 |
| 278.430(10) | 7.36(3) | ··· | ··· | 278 | g.s. |
| 281.262(15) | 2.14(2) | 2.14 [c] | 251 | 560 | 278 |
| 281.4(–) | ··· | <0.002 | 460 | 769 | 487 |
| 281.7(–) | ··· | 0.020(4) | 802 | 1112 | 830 |
| 342.54(–) | ··· | 0.11(1) | 460 | 830 | 487 |
| 342.88(–) | 0.640(5) | 0.53(3) | 741 | 1112 | 769 |
| 382.08(13) | 0.008(3) | 0.007(2) | 730 | 1112 | 730 |
| 415.88(13) | 0.008(4) | <0.012 | 817 | 1261 | 845 |
| 459.600(10) | 100.0 | ··· | ··· | 487 | 28 |
| 462.04(–) | ··· | <0.003 | 802 | 1292 | 830 |
| 487.390(20) | 18.43(4) | ··· | ··· | 487 | g.s. |
| 491.93(13) | 0.015(3) | 0.024(2) | 741 | 1261 | 769 |
| 531.831(20) | 1.14(1) | ··· | ··· | 560 | 28 |
| 551.50(–) | 0.064(6) | 0.031(2) | 251 | 830 | 278 |
| 551.98(–) | | 0.012(4) | 532 | 1112 | 560 |
| 560.053(25) | 0.079(4) | 0.076(8) | 460 | 1047 | 487 |
| 624.344(20) | 1.26(1) | 1.26 | 460 | 1112 | 487 |
| 701.10(15) | 0.017(4) | 0.014(5) | 532 | 1261 | 560 |
| 701.76(–) | 0.0003 [d] | ··· | ··· | 730 | 28 |
| 722.5(–) | ··· | ≤0.003 | 460 | 1210 | 487 |
| 729.57(2) | 0.016(4) | ··· | ··· | 730 | g.s. |
| 732.62(15) | 0.017(3) | 0.019(5) | 532 | 1292 | 560 |
| 740.96(2) | 0.486(9) | ··· | ··· | 769 | 28 |
| 768.77(–) | 0.064(6) | (0.055) [e] | ··· | 769 | g.s. |
| 769.01(–) | | 0.0093(9) | 251 | 1047 | 278 |
| 773.54(16) | 0.003(2) | 0.0053(14) | 460 | 1261 | 487 |
| 802.10(2) | 2.49(2) | ··· | ··· | 830 | 28 |
| 804.60(12) | 0.028(3) | 0.0195(14) | 460 | 1292 | 487 |
| 817.00(–) | <0.0008 | ··· | ··· | 845 | 28 |
| 829.93(2) | 0.083(2) | ··· | ··· | 830 | g.s. |
| 833.28(2) | 0.590(5) | 0.59 [c] | 251 | 1112 | 278 |
| 918.29(15) | 0.008(2) | <0.0008 | 251 | 1196 | 278 |
| 931.57(25) | 0.0027(12) | 0.0022(4) | 251 | 1210 | 278 |
| 982.27(2) | 0.208(4) | 0.208 [c] | 251 | 1261 | 278 |
| 1013.57(6) | 0.017(4) | 0.0064(6) | 251 | 1292 | 278 |
| 1019.43(4) | 0.029(7) | ··· | ··· | 1047 | 28 |
| 1083.85(2) | 6.4(1) | ··· | ··· | 1112 | 28 |
| 1111.64(2) | 2.48(6) | ··· | ··· | 1112 | g.s. |
| 1168.8(–) | ≤0.0006 | ··· | ··· | 1196 | 28 |
| 1181.96(10) | 0.0015(6) | ··· | ··· | 1210 | 28 |
| 1232.82(2) | 0.097(3) | ··· | ··· | 1261 | 28 |
| 1260.63(2) | 0.145(5) | ··· | ··· | 1261 | g.s. |
| 1264.16(2) | 0.106(2) | ··· | ··· | 1292 | 28 |
| 1291.50(13) | 0.0036(5) | ··· | ··· | 1292 | g.s. |

[a] The errors quoted reflect only the precision of peak location by our computer fitting code. For the absolute energies a 50-eV error should be added in quadrature to account for system nonlinearities and energy standard uncertainties.

[b] The quoted errors reflect only the statistical accuracy of the peak area determinations. A 3% error should be added in quadrature to account for uncertainties in the detector efficiency calibrations.

[c] These $\gamma$-ray intensities were used for calibration of the detector efficiencies in the coincidence system.

[d] This intensity is deduced from the 730 keV intensity and the known branching ratio of decay from the 730-keV level.

[e] This is the difference between the unresolved 769-keV doublet intensity from singles and the 769.01 keV intensity from coincidence data.

studies.

The singles studies were carried out with the CSS system to observe weak $\gamma$ rays and with a 40-$cm^3$ detector, whose efficiency function is well known, to obtain relative intensity values. Impurities in the Te target gave rise to a number of radioactive nuclides including $^{131}I$, $^{110}Ag$, $^{121}Te$, and $^{160}Tb$ whose $\gamma$-ray energies are well known. Counting the unpurified source alone on several detectors, as well as with a group of primary standards, provided the data for a precise energy calibration. Those $\gamma$ rays attributed solely to $^{129}Te^m$ decay are shown in Table II.

For coincidence studies three source-detector

TABLE II. $\gamma$-ray energies and intensities following decay of $^{129}Te^m$.

| $E_\gamma(\Delta E_\gamma)$ (keV) [a] | $I_\gamma(\Delta I_\gamma)$ Singles [b] | Coincidence | Coinc. gate (keV) | Assignment | |
|---|---|---|---|---|---|
| 27.814 | ... | ... | ... | 28 | g.s. |
| 76.10 | ... | 0.0068(15) | 741 | 845 | 769 |
| 115.30(15) | 0.008(2) | 0.0058(17) | 730 | 845 | 730 |
| 208.960(–) | 0.006 [c] | ... | ... | 487 | 278 |
| 242.2(–) | 0.004(2) | 0.014(2) | 460 | 730 | 487 |
| 250.615(15) | 0.0063 [c] | ... | ... | 278 | 28 |
| 278.430(–) | 0.0093 [c] | ... | ... | 278 | g.s. |
| 281.38(–) | ... | <0.002 | 460 | 769 | 487 |
| 281.44 (–) | ... | 0.011(1) | 741 | 1050 | 769 |
| 320.64(10) | 0.014(3) | 0.013(2) | 730 | 1050 | 730 |
| 357.48(–) | ≤0.003 | <0.005 | 460 | 845 | 487 |
| 459.600(–) | 0.026 [c] | ... | ... | 487 | 28 |
| 487.390(–) | 0.005 [c] | ... | ... | 487 | g.s. |
| 490.34(–) | ... | <0.005 | 251 | 769 | 278 |
| 552.43(–) | 0.005(4) [d] | 0.006(2) | 730 | 1282 | 730 |
| 556.652(–) | 2.52(3) | 2.52 | 817 | 1401 | 845 |
| 562.82(–) | ... | ≤0.01 | 460 | 1050 | 487 |
| 671.84(2) | 0.53(1) | 0.53 | 730 | 1401 | 730 |
| 695.882(20) | 63.85(25) | ... | ... | 696 | g.s. |
| 701.7(3) | 0.53(1) | ... | ... | 730 | 28 |
| 705.52(4) | 0.11(1) | 0.11(2) | 696 | 1401 | 696 |
| 716.60(15) | 0.005(3) | ≤0.005 | 460 | 1204 | 487 |
| 729.57(2) | 14.9(1) | ... | ... | 730 | g.s. |
| 740.96(2) | 0.58(1) [d] | ... | ... | 769 | 28 |
| 768.77(2) | 0.060(b) [d] | | ... | 769 | g.s. |
| 771.80(15) | 0.009(3) | 0.0063(7) | 251 | 1050 | 278 |
| 794.60(20) | 0.013(3) | 0.011(2) | 460 | 1282 | 487 |
| 817.04(2) | 1.94(2) | ... | ... | 845 | 28 |
| 844.81(2) | 0.73(3) | ... | ... | 845 | g.s. |
| 924.5(–) | ... | <0.0013 | 251 | 1204 | 278 |
| 1003.65(8) | 0.015(3) | 0.007(16) | 251 | 1282 | 278 |
| 1022.43(2) | 0.37(2) | ... | ... | 1050 | 28 |
| 1050.21(2) | 0.38(3) | ... | ... | 1050 | g.s. |
| 1176.0(5) | 0.002(1) | ... | ... | 1204 | 28 |
| 1203.59(10) | 0.005(1) | ... | ... | 1204 | g.s. |
| 1254.13(6) | 0.009(1) | ... | ... | 1282 | 28 |
| 1281.96(10) | 0.0046(8) | ... | ... | 1281 | g.s. |
| 1373.75(8) | 0.0057(6) | ... | ... | 1401 | 28 |
| 1401.36(3) | 0.074(1) | ... | ... | 1401 | g.s. |

[a] The errors quoted reflect only the precision of peak location by our computer fitting code. For the absolute energies a 50-eV error should be added in quadrature to account for system nonlinearities and energy standard uncertainties.

[b] The quoted errors reflect only the statistical accuracy of the peak area determinations. A 3% error should be added in quadrature to account for uncertainties in the detector efficiency calibrations.

[c] These intensities are deduced from the observed $\gamma$-ray intensities into the parent level and the known decay branching.

[d] This intensity is the difference between that observed in an equilibrium source and the intensity of an unresolved $\gamma$ ray from the Te ground state decay. (See Table I.)

geometries, representing a variety of compromises between large detector solid angles and most effective shielding against interdetector scattering, were used. A 180° geometry with the detectors separated by 6.4 mm of W or Pb shielding and with the source axially located in a hole in the shield gave the best sensitivity for weak $\gamma$-ray cascades. Coincidence rates varied from $\lesssim 50$/s in the low geometry well-shielded case to ~300/s in the closest geometry. True/chance ratios varied from about 2 in the former to greater than 10 in the latter cases. Roughly 4 $(10)^7$ coincidences were accumulated in each geometry.

All the $\gamma$-ray energy data used for level energy determinations were taken from the single detector work, hence only a crude energy calibration of the coincidence detectors was needed. This was obtained for each detector by using the four $\gamma$ rays at 209.0, 281.3, 833.3, and 982.4 keV that populate the 278.4-keV level. The observed coincidence rates with the 250.6-keV $\gamma$ ray were used to obtain efficiency curves. Any energy dependence of the electronics coincidence efficiency would be reflected in these curves. No correction, however, is possible for angular correlation effects.

Figure 3 shows coincidence data for a few of the more interesting gates. The gate at 460 keV clearly shows that a 560-keV $\gamma$ ray populates the 487-keV level. The 560-keV intensity in this spectrum was obtained accurately (apart from angular correlation effects) by direct comparison with the nearby intense 624-keV $\gamma$ ray that also populates the 487-keV level. Data were obtained at both 180° and 90° detector geometries. Although statistics were much worse at 90°, the 560-keV intensity relative to the 624-keV intensity was significantly greater than at 180° ($0.133 \pm 0.025$ vs $0.073 \pm 0.006$ on the intensity scale of Tables I and II). This implies a 90°/180° anisotropy for the 560-460 cascade of $1.68 \pm 0.34$, very similar to that measured by DeRaedt *et al.* for the 343-460 ($\frac{3}{2}$-$\frac{5}{2}$-$\frac{5}{2}$) cascade.[6] Any anisotropy greater than 1.35 would preclude a spin of $\frac{5}{2}$ for the 1047-keV level.

Two weak low-energy $\gamma$ rays of 115.3 and 76.1 keV that depopulate the level at 844.8 keV were detected in coincidence with the 730- and 741 keV $\gamma$ rays, respectively. More definitive evidence for these $\gamma$ rays is the appearance of the 556.7-keV $\gamma$ ray (that populates the 844.8-keV level) in coincidence with the 730- and 741-keV $\gamma$ rays.

All the coincidence results are summarized in Tables I and II. The listed intensity errors do not include possible angular correlation effects. Those intensities listed without error were normalized to the singles data.

## III. THE DECAY SCHEMES

The new decay schemes are presented in Figs. 4 and 5. The most significant discrepancy between the earlier decay work and the ($^3$He, $d$) studies concerned the clear $l=2$ assignment for a level at 1050 keV, whereas the 1050-keV level observed in the decay studies was clearly $\frac{7}{2}^+$ or $\frac{9}{2}^+$ as it is fed by the $\beta$ decay of $\frac{11}{2}^-$ $^{129}$Te$^{m}$ and decays to the $\frac{7}{2}^+$ and $\frac{5}{2}^+$ ground and 28-keV states, respectively. This inconsistency has been removed by the discovery of a $\frac{3}{2}^+$ level at 1047.44 keV[4-6] that decays by three $\gamma$ rays to $\frac{5}{2}^+$ levels at 27.8 and 487.4 keV and a $\frac{3}{2}^+$ level at 278.4 keV.

We suggest that the 1401.4-keV level has a $J^{\pi}$ value of $\frac{11}{2}^-$. In earlier radioactive decay studies both Berzins *et al.*[2] and Dickinson *et al.*[3] made tentative $\frac{9}{2}^+$ assignments for the 1401.4-keV level

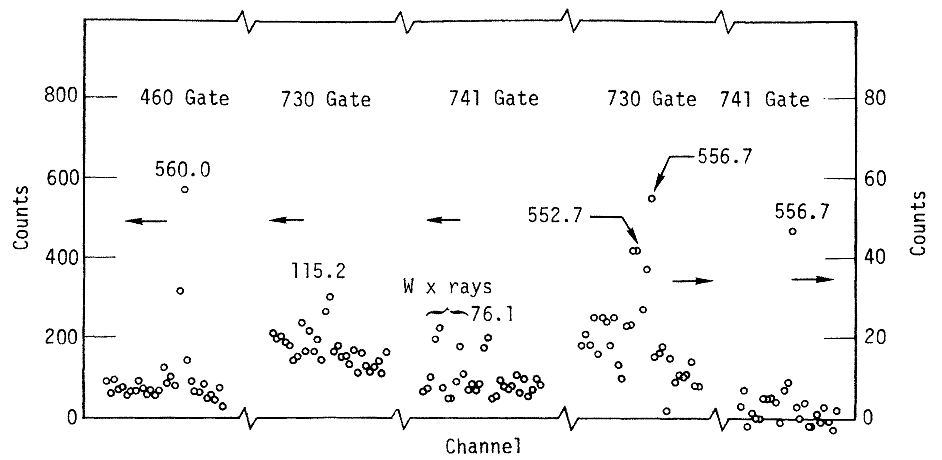

FIG. 3. $\gamma$-ray spectra in coincidence with selected gate energies (in keV). Data that support the placement of the 560-keV $\gamma$ ray and the 115.2- and 76.1-keV $\gamma$ rays are shown. The abscissa is about 1.4 keV/channel. Coincidences resulting from chance and from Compton continuum under the gated peak have been subtracted.

that is fed with a log*ft* value of 8.4 by the $\frac{11}{2}^-$ $^{129}$Te$^m$ isomer, and decays weakly to the $\frac{7}{2}^+$ and $\frac{5}{2}^+$ ground and first excited states. The ($^3$He, *d*) studies revealed a tentative $l=5$ assignment for this level and a tentative $\frac{11}{2}^-$ assignment was suggested. We have observed no new transitions from that state to other $\frac{5}{2}^+$ or $\frac{7}{2}^+$ states. We have examined the *E*1, *M*2, and *E*3 branching from the 1401.4-keV level and compared it with similar branching in $^{125}$Sb, $^{131}$I, $^{137}$La, and $^{139}$Pr. The results are shown in Fig. 6 and are quite consistent with an $\frac{11}{2}^-$ assignment for the 1401-keV level.

Dickinson *et al.*[3] identified the levels at 1203.7 and 1282.0 keV as low-spin levels on the basis of their branching to several $\frac{5}{2}^+$ states and suggested they were populated in the $\beta$ decay of $\frac{3}{2}^+$ $^{129}$Te$^g$. We were unable to observe these levels in our study of $^{129}$Te$^g$ and have assigned them to the $\beta$ decay of $\frac{11}{2}^-$ $^{129}$Te$^m$. The 1282.0-keV level is clearly a $\frac{7}{2}^+$ level as it is fed directly by $\beta$ decay and has a $\gamma$-ray branch to the $\frac{3}{2}^+$ level at 278.4 keV. The 1203.7-keV level is also assigned tentatively as $\frac{7}{2}^+$, although $\frac{9}{2}^+$ cannot be ruled out.

A level near 1210 keV with $l=0$ was observed in the ($^3$He, *d*) studies. In the decay of $\frac{3}{2}^+$ $^{129}$Te$^g$ we observe at 1209.9 keV a level whose decay prop-

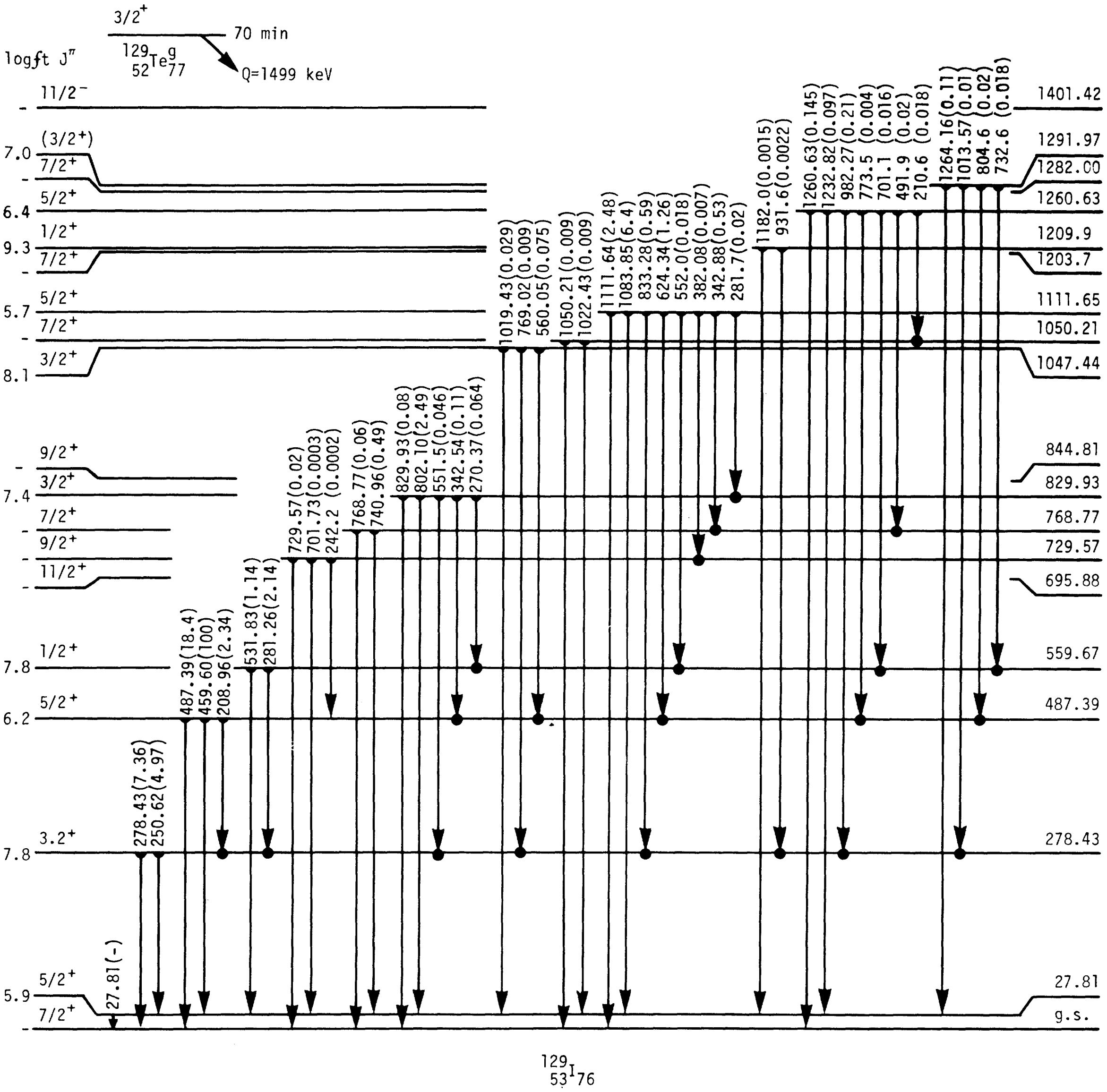

FIG. 4. Decay of $^{129}$Te$^g$. Energies are in keV. Relative $\gamma$-ray intensities are in parentheses. Those $\gamma$ rays seen in coincidence are denoted by a dot at the arrow head.

erties are consistent with the $\frac{1}{2}^{+}$ assignment required by $l=0$ transfer.

The level at 1292.0 keV can be $\frac{1}{2}^{+}$, $\frac{3}{2}^{+}$, or $\frac{5}{2}^{+}$ as it is fed by the $\frac{3}{2}^{+}$ $^{129}$Te$^{g}$ isomer. This level exhibits $\gamma$-ray branches to $\frac{1}{2}^{+}$, $\frac{3}{2}^{+}$, and $\frac{5}{2}^{+}$ levels, but not to $\frac{7}{2}^{+}$ levels. Because of the strength of branching to the $\frac{5}{2}^{+}$ levels, we favor a $\frac{3}{2}^{+}$ assignment for the 1292-keV level. Although the $\frac{1}{2}^{+}$ assignment cannot be ruled out by the strong branching to the $\frac{5}{2}^{+}$ states, the absence of an $l=0$ transition to the 1292.0-keV level in the ($^{3}$He, $d$) reaction suggests a $\frac{3}{2}^{+}$ or $\frac{5}{2}^{+}$ rather than a $\frac{1}{2}^{+}$ assignment. Because of the high transmission coefficient and strong forward peaking for $l=0$ transfer, such transitions are easily observed even for states with very small single-particle character.

The spin assignment for the 559.67-keV level has proven difficult to determine. Both Dickinson *et al.*[3] and Berzins *et al.*[2] suggested $\frac{3}{2}^{+}$ assignments for this level as they assigned an approximately 560-keV $\gamma$ ray as a transition between this level and the $\frac{7}{2}^{+}$ ground state, eliminating a $\frac{1}{2}^{+}$ assignment. However, a spin of $\frac{1}{2}$ is suggested by the ($^{3}$He, $d$) studies of Auble, Ball, and Fulmer[9] that

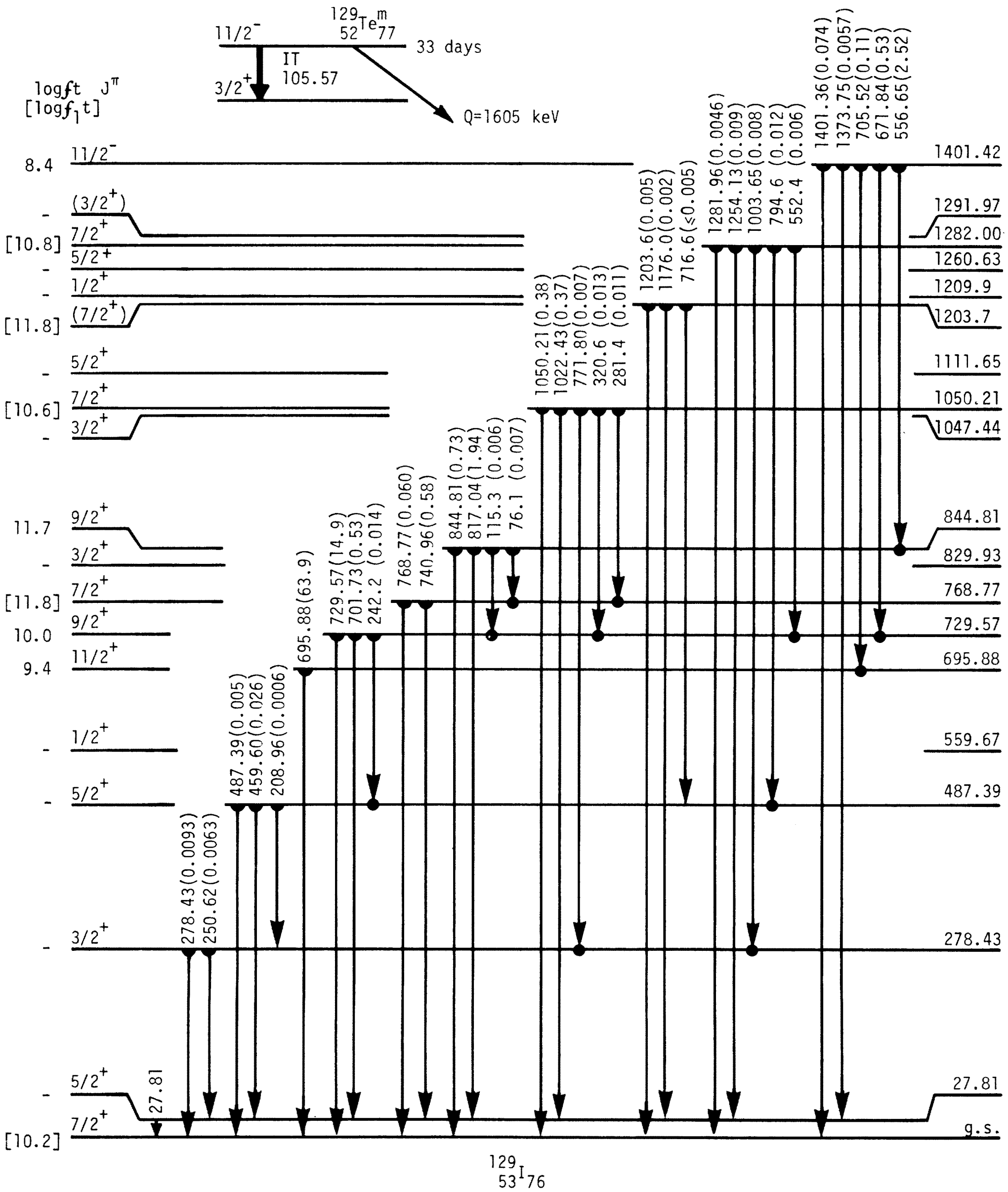

FIG. 5. Decay of $^{129}$Te$^{m}$. (See Fig. 4 caption.)

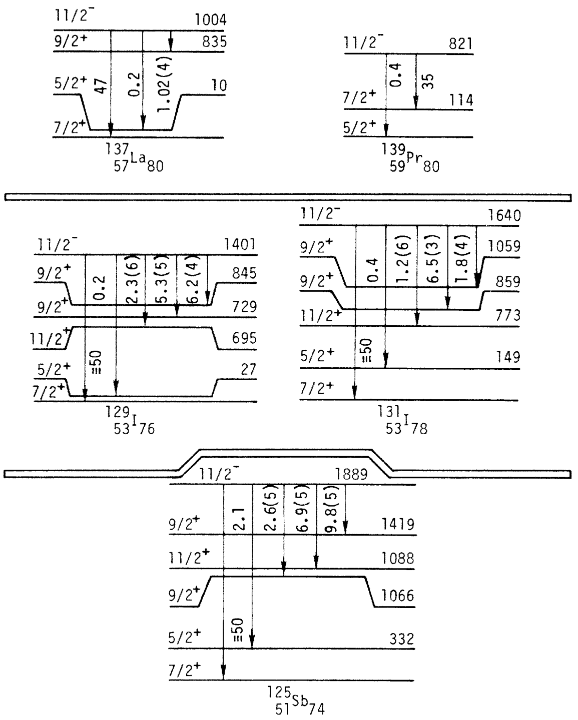

FIG. 6. Systematics of the $\frac{11}{2}^-$ state in odd-proton nuclei above the 50-proton closed shell. Hindrance factors for the lowest order multipole are shown for each transition, based on the hindrance of the $\frac{11}{2}^-$ to $\frac{7}{2}^+$ $M2$ transition. This $M2$ transition has been measured for La and Pr, and we have assumed a hindrance value of 50 in the other nuclides.

clearly show the presence of an $l=0$ transition to a level at 560 ± 5 keV. Careful reexamination of the energies observed by Dickinson *et al.* indicated that the 560-keV $\gamma$-ray energy was not consistent with the sum of the 532- and 28-keV $\gamma$ rays.[10] However, a measurement by DeRaedt *et al.*[6] disagreed with that conclusion. Silverans, Schoeters, and Vanneste[7] have recently reported the measurement of anisotropies for a number of $\gamma$ rays following decay of oriented $^{129}$Te nuclei. They reported an anisotropy value for the 278-281 peak of 0.001 ± 0.027, a value difficult to interpret as it includes both the 281-keV $\gamma$ ray from the 559.67-keV level in question and the 278-keV $\gamma$ ray from the $\frac{3}{2}^+$ level at that energy. Silverans *et al.* do not report an anisotropy value directly for the 532-keV $\gamma$ ray but indicate $U_2F_2$ possibilities over a rather wide range of values (0.30 to 0.62). They interpret the presence of any anisotropy as eliminating the $\frac{1}{2}^+$ spin possibility. We have clearly determined that the 560.05-keV $\gamma$ ray does not have the correct energy to fit between ground and the 559.67-keV level. We have also shown that most, if not all, of the 560-keV intensity occurs in coincidence with decay of the 487-keV level. DeRaedt *et al.*, on the other hand, found only about $\frac{1}{3}$ of the 560-keV peak in coincidence with the 487-keV decay. We can find no evidence for a second $\gamma$-ray component in the 560-keV peak to connect the 559.67-keV level to ground. We see no evidence for a second level near 560 keV and suggest there is only one such

TABLE III. Values of $B(E2)$ in $^{129}$I, in units of $e^2\text{cm}^4\times10^{-50}$. See text for the source of the experimental numbers.

| | | Theory | | |
|---|---|---|---|---|
| $2J_i/2J_f$ | Experiment | 3-particle Cluster phonon model [a] | particle phonon model [b] | Quasiparticle phonon model [c] |
| $5_1/7_1$ | 9.78 ± 0.85 | 8.9 | 1.8 | 2.2 |
| $3_1/7_1$ | 7.0 | 12.9 | 12.7 | 21.5 [d] |
| $3_1/5_1$ | 1.8 ± 0.7 or<br>7.4 ± 0.9 | 4.2 | 860 | 4.0 [d] |
| $5_2/7_1$ | 2.1 | 5.3 | 0.48 | |
| $5_2/5_1$ | <0.1 | 0.4 | 0.57 | |
| $11_1/7_1$ | 8.1 | 9.7 | 8.0 | |
| $9_1/7_1$ | 6.2 | 3.8 | 3.8 | |
| $9_1/5_1$ | 2.7 ± 1.0 or<br>0.35 ± 0.04 | 2.6 | 0.94 | |
| $7_2/7_1$ | 1.1 | 0.24 | 0.070 | |
| $3_2/7_1$ | 0.8 | | 0.088 | |
| $9_2/7_1$ | 1.2 | | 0.15 | |
| $9_2/5_1$ | >3.0 | | 5.2 | |
| $7_3/7_1$ | 0.8 | | 4.1 | |

[a] Reference 14.
[b] Reference 13.
[c] Reference 22.
[d] Values for $^{127}$I.

level, a level at 559.67 keV. As the $l=0$ character from the ($^3$He,*d*) studies is unmistakable, the 559.67-keV level must have a spin and partiy of $\frac{1}{2}^+$. This assignment is not consistent with the observed anisotropy for the 532-keV $\gamma$ ray. However, Silverans *et al.* pointed out that this was a weak peak, and it seems possible, therefore, that effects such as Compton background or 281 plus 250 summing might account for the observed asymmetry.

For several of the remaining levels, considerable agreement exists for the spin and parity assignments among the ($^3$He,*d*) studies, the angular correlation studies, the orientation studies, the Coulomb excitation studies, and our work. These include the $\frac{3}{2}^+$ level at 278 keV, the $\frac{5}{2}^+$ levels at 487 and 1112 keV, the $\frac{11}{2}^+$ level at 696 keV, the $\frac{9}{2}^+$ level at 730 keV, and the $\frac{7}{2}^+$ level at 769 keV. Once the 1401-keV level is established as $\frac{11}{2}^-$, the 845-keV level must be $\frac{9}{2}$ or greater. The 845-keV level also feeds the $\frac{5}{2}^+$ level at 28 keV, hence must be $\frac{9}{2}^+$ or less, thus establishing it as a $\frac{9}{2}^+$ level. The $\frac{3}{2}^+$ assignments at 1047 and 1292 keV and the $\frac{7}{2}^+$ assignment at 1204 keV are less certain. However, the angular dependence of our coincidence data for the 560-460 cascade clearly

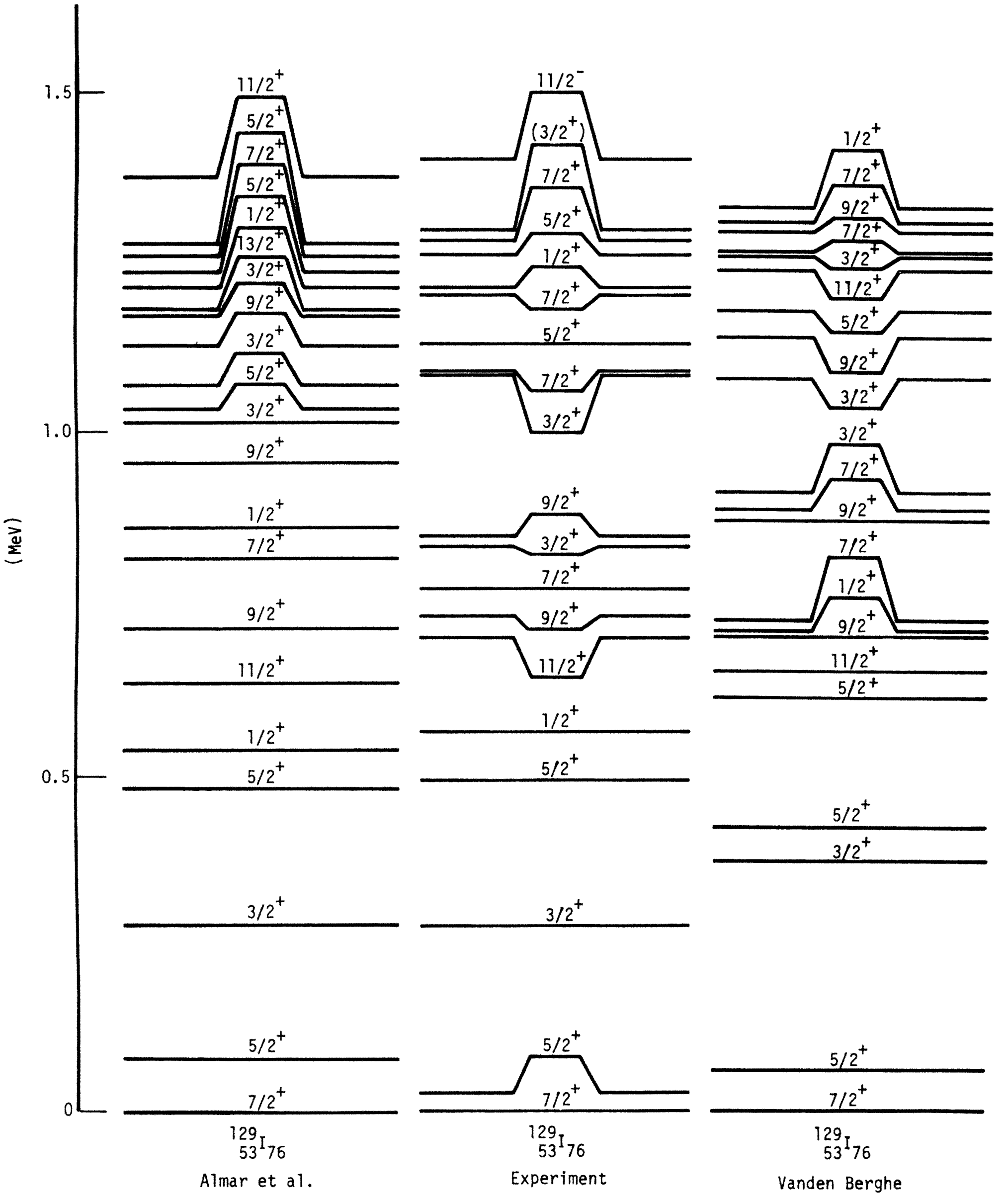

FIG. 7. Calculated and experimental level structure of $^{129}$I. The calculations are from Refs. 13 and 14.

favors a spin of $\frac{3}{2}$ for the 1047-keV level. The $\frac{5}{2}^+$ assignment for the 1261-keV level is made with some certainty. This level is populated by an $l=2$ transition in the ($^3$He, $d$) reaction, fed strongly in $\beta$ decay from $^{129}$Te$^g$, and decays to levels with spins $\frac{7}{2}$, $\frac{5}{2}$, $\frac{3}{2}$, and the 559.67-keV $\frac{1}{2}^+$ state. Most important are the strong reduced transition probabilities to the $\frac{7}{2}^+$ states at 769 and 1050 keV. Were these transitions to be pure $E2$ from a $\frac{3}{2}^+$ level, their $B(E2)$ values would be very high relative to the ground state transition.

We also note the presence of two low-energy transitions from the $\frac{9}{2}^+$ level at 845 keV to the $\frac{7}{2}^+$ level at 769 keV and the $\frac{9}{2}^+$ level at 729 keV. The $B(E2)$ value for the 845-keV $\gamma$ ray is 3.1 times the single-particle estimate.[8] Therefore, these two low-energy transitions must be largely $M1$, otherwise their $B(E2)_{\mathrm{exp}}/B(E2)_{\mathrm{s.p.}}$ ratios would be very large ($\gtrsim 5000$ and $\gtrsim 600$ for the 76 and 115 keV, respectively). This same 845-keV level is also the one fed most strongly by the $h_{11/2}$ level at 1401 keV. These data suggest that the 845-keV level has a small but significant contribution from the 1-hole 4-particle state involving one hole in the $g_{9/2}$ proton shell below $Z=50$.

## IV. DISCUSSION

For the structure of iodine nuclei, the simple particle-vibration model used by Kisslinger and Sorenson[11,12] failed on several points. First, it did not account for the systematic occurrence of a second low-lying $\frac{5}{2}^+$ level in all of the odd-mass iodine nuclei; second, it did not account for the large $B(E2)$ observed in the $\frac{5}{2}{}_1^+ \rightarrow \frac{7}{2}{}_1^+$ transition by Bemis and Fransson[1]; and third, it did not account for the large number of levels observed at an excitation energy of 1 to 3 MeV. The situation was improved when calculations based on the suggestions of Alaga, Paar, and co-workers[23-26] were undertaken. These calculations introduce the effects of three-particle clustering in nuclei such as iodine.

Table III lists a number of $B(E2)$ values for $^{129}$I obtained from the Coulomb excitation work of Renwick *et al.*,[8] the conversion electron measurements of the $\frac{5}{2}{}_1$ to $\frac{7}{2}{}_1$ transition by Bemis and Fransson,[1] the $\gamma$-ray multipolarity determinations of Silverans *et al.*[7] and of DeRaedt *et al.*,[6] and the present work. The data are compared with calculations based on a single-particle or quasiparticle phonon model and on a three-particle cluster phonon model.[13,14,22] The latter model gives excellent agreement with experiments for the $\frac{5}{2}{}_1$ to $\frac{7}{2}{}_1$ transition, and there is some overall improvement for the other transitions.

Figure 7 shows a comparison between the $^{129}$I experimental level structure and two calculated level structures based on the three-particle cluster-phonon model. There is good agreement between the position and number of levels predicted for $^{129}$I and those that are found experimentally.

We have discussed elsewhere the desirability of a model including both particle plus core and cluster configurations (Jackson *et al.*[27,28]). We noted the general trend of levels indicated a sensitivity to the energies of the states of the adjacent even-even Te core and hence a particle plus Te core description. Specifically, the $B(E2)$ values for the Coulomb excitation of many $^{129}$I states are closely related to the $B(E2)$ value for the Coulomb excitation of the $2_1^+$ state in $^{128}$Te. However, the presence and spectroscopy of a second low-lying $\frac{5}{2}^+$ state pointed to the need for including three-particle cluster configurations. In particular, Parsa, Gordon, and Walters[29] noted the near constant separation of the two low-lying $\frac{5}{2}^+$ states in I nuclides with $125 \leqslant A \leqslant 135$. New evidence for the latter configurations is displayed in Fig. 8, where we show the four low-lying $\frac{5}{2}^+$ states in odd-mass

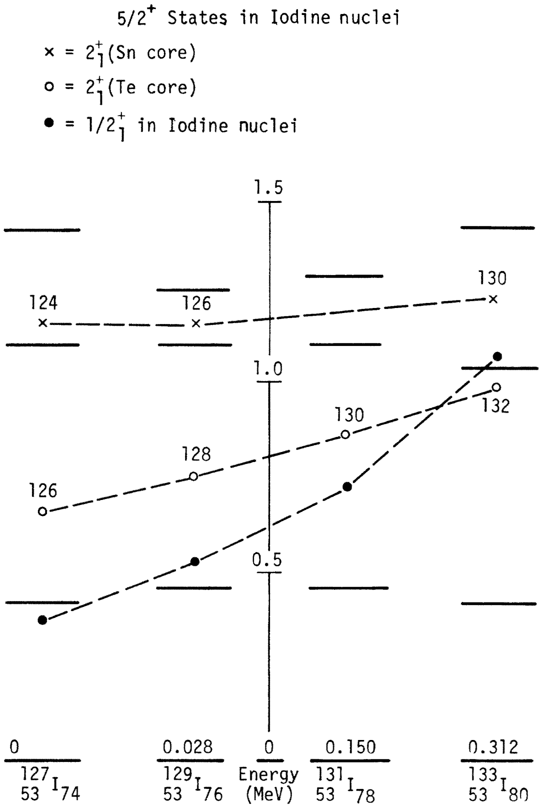

FIG. 8. Systematics of the $\frac{5}{2}^+$ states in I nuclides compared with the first $2^+$ states in the neighboring Te and Sn cores and with the first $\frac{1}{2}^+$ states in I.

I nuclides plotted with the energies of the appropriate even-even Sn core. The higher-lying levels were distinguished by their similarities in $\beta$ feeding and $\gamma$ branching. For these $\frac{5}{2}^+$ states, it appears that the cluster plus Sn core is a more appropriate description than the particle plus Te core. On the other hand, the particle plus Te core configuration appears more appropriate for most other states (the $\frac{1}{2}^+$ shown in Fig. 8 is but one example). Recent calculations utilizing "dressed" three-quasiparticle calculations[30] have also reproduced the $B(E2)$ values for the $\frac{5}{2}^+_1$ to $\frac{7}{2}^+_1$ transition. It is to be hoped that these calculations will be performed for additional levels and transitions, as this model agrees with experimental results in a number of diverse nuclei.

In our coincidence studies, we have observed and established the positions of four low-intensity $\gamma$ rays with energies of 76.1, 115.3, 281.6, and 320.6 keV. These $\gamma$ rays correspond to transitions from the $\frac{9}{2}^+_2$ and $\frac{7}{2}^+_3$ to the $\frac{9}{2}^+_1$ and $\frac{7}{2}^+_2$ levels. In the particle-plus-core models, these levels all belong to the multiplet obtained by coupling the $g_{7/2}$ and $d_{5/2}$ states to the $^{128}$Te core. The $B(E2)$ values for transitions to all four of these levels have been determined by Coulomb excitation studies. These values and our $\gamma$-ray branching ratios limit the multipolarities to be largely $M1$ in character. These transition probabilities offer a sensitive test for any calculated wave functions.

This work was performed under the auspices of the U.S. Energy Research and Development Administration under Contract No. W-7405-Eng-48.

---

*Consultant to Lawrence Livermore Laboratory, Permanent address: University of Maryland, College Park, Maryland 20742.

[1] C. E. Bemis and K. Fransson, Phys. Lett. 19, 567 (1965).

[2] G. Berzins, L. M. Beyer, W. H. Kelly, W. B. Walters, and G. E. Gordon, Nucl. Phys. A93, 456 (1967).

[3] W. C. Dickinson, S. D. Bloom, and L. G. Mann, Nucl. Phys. A123, 481 (1969).

[4] W. B. Walters and R. A. Meyer, Bull. Am. Phys. Soc. 17, 907 (1972).

[5] L. G. Mann, W. B. Walters, and R. A. Meyer, Bull. Am. Phys. Soc. 18, 1425 (1973).

[6] J. DeRaedt, M. Rots, and H. Van de Voorde, Phys. Rev. C 9, 2391 (1974).

[7] R. E. Silverans, E. Schoeters, and L. Vanneste, Nucl. Phys. A204, 625 (1973).

[8] B. W. Renwick, B. Byrne, D. A. Eastham, P. D. Forsyth, and D. G. E. Martin, Nucl. Phys. A208, (1973).

[9] R. L. Auble, J. B. Ball, and C. B. Fulmer, Phys. Rev. 169, 955 (1968).

[10] D. J. Horen, Nucl. Data B8, 123 (1972).

[11] L. S. Kisslinger and R. A. Sorensen, Rev. Mod. Phys. 35, 853 (1963).

[12] K. Heyde and P. J. Brussaard, Nucl. Phys. A104, 81 (1967).

[13] M. L. Rustgi, J. G. Lucas, and S. N. Mukherjee, Nucl. Phys. A117, 321 (1968).

[14] R. Almar, O. Civitarese, and F. Krmpotić, Phys. Rev. C 8, 1518 (1973).

[15] G. Vanden Berghe, Z. Phys. 266, 139 (1974); private communication.

[16] A. Kuriyama, T. Marumori, K. Matsuyanagi, and R. Okamata, Prog. Theor. Phys. Suppl. 58, 1 (1975).

[17] R. A. Meyer, in *Problems of Vibrational Nuclei,* edited by G. Alaga, V. Paar, and L. Sips (North-Holland, Amsterdam, 1975), Chap. 7.

[18] J. B. Niday and L. G. Mann, in *Proceedings of the International Conference on Radioactivity in Nuclear Spectroscopy, Vanderbilt University, Nashville, Tennessee, 1969,* edited by J. H. Hamilton and J. C. Manthuruthil (Gordon and Breach, New York, 1972), Vol. I, p. 313.

[19] An alternative approach, using a movable head disk, requires much larger core buffering in order to compensate for the longer track switching times. The cost of core memory has dropped in recent years to the point where this approach is undoubtedly the most practical today. J. P. Gonidec, Nucl. Instrum. Methods 88, 125 (1970); J. W. D. Sinclair, J. W. Smith, C. M. Rozsa, and S. L. Blatt, *ibid.* 111, 61 (1973).

[20] R. Gunnink and J. B. Niday, Report No. UCRL-51061, 1972 (unpublished).

[21] D. C. Camp, in *Proceedings of the International Conference on Radioactivity in Nuclear Spectroscopy, Vanderbilt University, Nashville, Tennessee, 1969* (see Ref. 18), Vol. I, p. 135.

[22] B. S. Reehal and R. A. Sorensen, Phys. Rev. C 2, 819 (1970).

[23] G. Alaga and G. Ialongo, Nucl. Phys. A97, 600 (1965).

[24] V. Paar, Phys. Lett. B39, 466 (1972).

[25] V. Paar, Phys. Lett. B39, 587 (1972).

[26] V. Paar, Nucl. Phys. A211, 29 (1973).

[27] S. V. Jackson, W. B. Walters, and R. A. Meyer, Phys. Rev. C 11, 1323 (1975).

[28] S. V. Jackson, Report No. UCRL-51846 (unpublished), 1975 Ph.D. thesis.

[29] B. Parsa, G. E. Gordon, and W. B. Walters, Nucl. Phys. A110, 679 (1968).

[30] A. Kuriyama, T. Marumori, and K. Matsuyanagi, Prog. Theor. Phys. 51m, 779 (1974).